

# APPLICATIONS BULLETIN

## Finer particle size allows better coating characterisation with the Calotest

### Introduction

Although the CSM Calotest is now an established method for the determination of coating thickness, it can also be applied to a variety of related applications and used to gain further information from other complimentary test methods. A selection are presented in this application note.

### Applications

Present trials using a new type of diamond paste with a particle size < 1  $\mu$ m have shown a net improvement in the quality of craters produced with the Calotest. This is particularly evident in the case of very thin coatings such as those shown in Fig. 1, where the use of larger particle sizes causes smearing of one layer into another resulting in reduced contrast and difficulties in accurately determining crater dimensions and quantitative film thickness values.

The Calotest can also be used to investigate track paths produced in routine scratch adhesion tests and pin-on-disk tribometer tests, where additional information can be gained which is inaccessible via other methods.

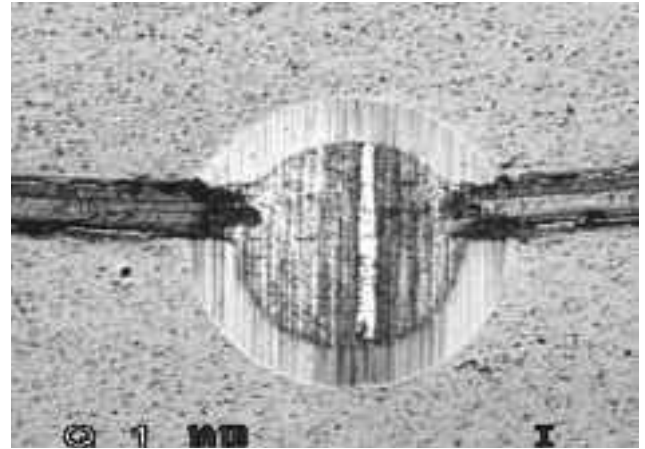


**Figure 2 :** Calotest crater made over a pin-on-disk tribometer wear track (test conditions; 5 N load, 10 cms-1 speed, 1 hour, ball diameter = 20 mm). Sample is TiAlN deposited onto a 100Cr6 substrate.

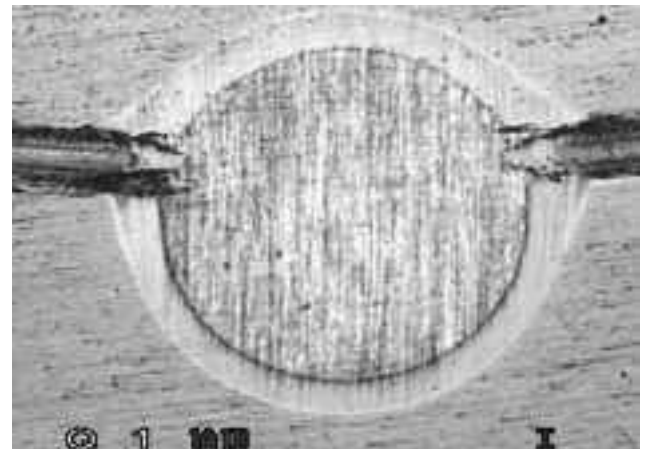


**Figure 3 :** Calotest crater made over a pin-on-disk tribometer wear track (test conditions; 5 N load, 10 cms-1 speed, 1 hour, ball diameter = 25.4 mm). Sample is TiAlN deposited onto a 100Cr6 substrate

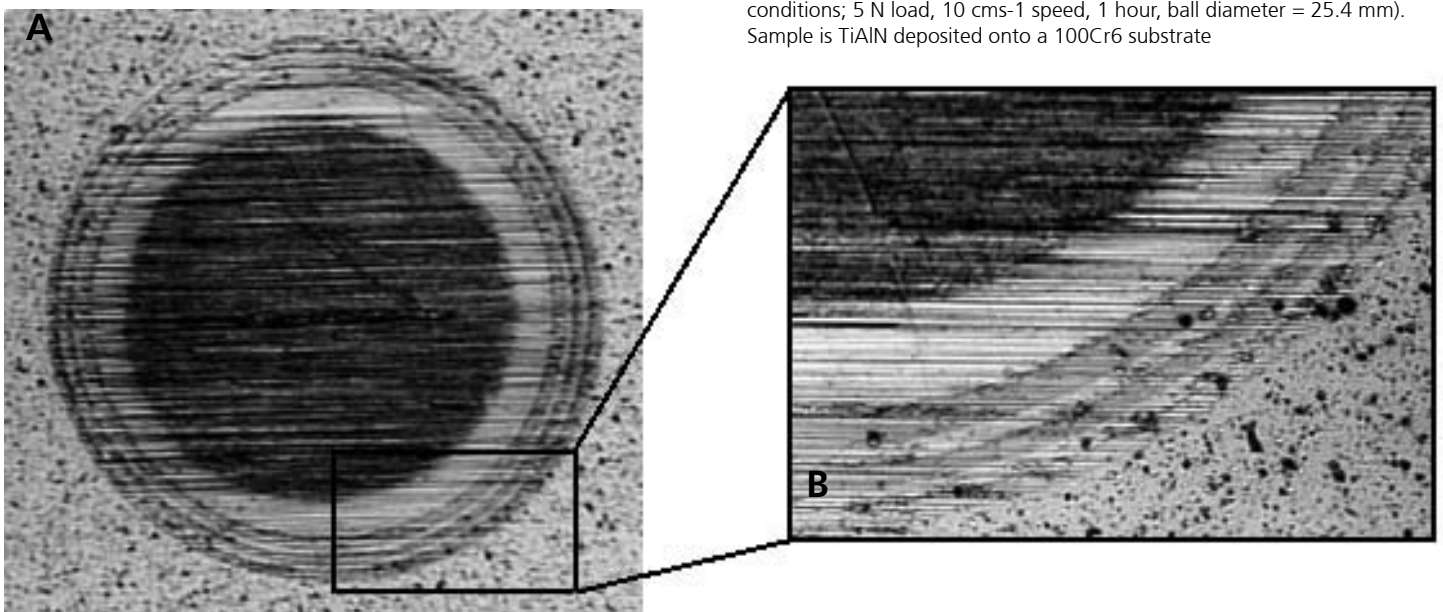


**Figure 1 :** Calotest performed on a multilayered coating made up of alternate TiN/TiCN deposited on a standard AISI 440C steel substrate (a). The close-up (b) shows that even very thin layers (in this case having a thickness of approximately 250 nm) can be accurately measured with this method.

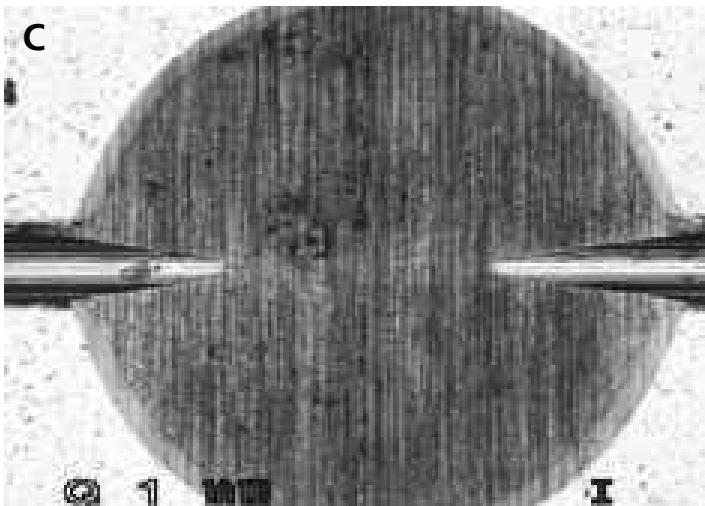
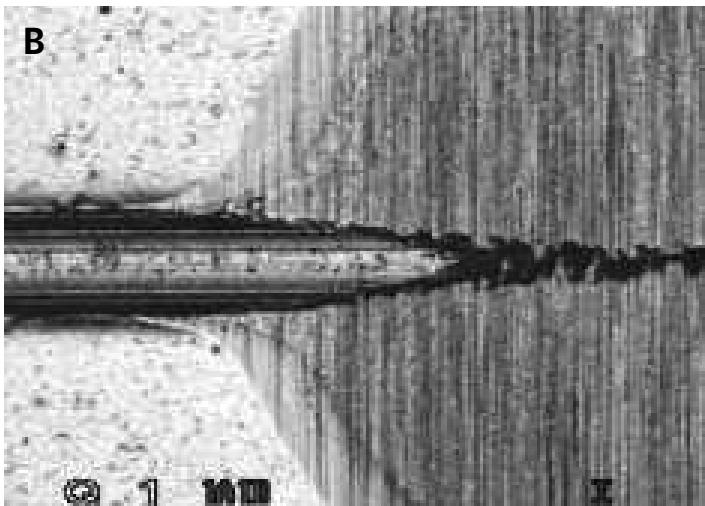
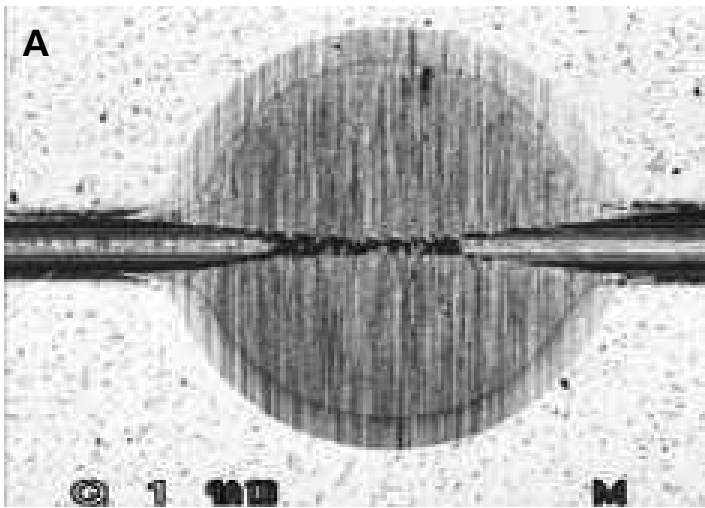


**Figure 4** : Calotest craters produced on a RVT scratch track made on a TiN-coated steel sample (test conditions; 0-100 N progressive loading, 10 mm/min. speed, 200 m tip radius). The critical load (46.7 N) occurred in the central area of the crater. Micrograph (b) is a zoomed image of the left hand portion of (a), whereas (c) shows a deeper crater to below the scratch track.

Figs. 2 and 3 show typical Calotest craters produced over pin-on-disk wear tracks. Conventionally, the volume of worn material is calculated by measuring across the wear track with a stylus profilometer, but this gives little information concerning the actual wear mechanism encountered. For coated systems, the crater can shed light on the wear and plastic deformation of the coating, and can often confirm

that plastic deformation occurs in the softer substrate and should thus be accounted for in the coating wear results. In addition, the depth of the wear track can be estimated, as can the coating thickness, and variations in the sphericity of the crater can be attributed to deformation at the edges of the wear track (see Fig. 3).

For scratch adhesion tests on coated samples, the Calotest can be used to investigate failure mechanisms as well as the scratch depth at various critical points along its path. The example shown in Fig. 4 (a) shows a crater made over the zone of critical failure for a TiN coating on a 440C substrate. The left hand side is the track before total failure, whereas the right hand side is the track after. A close-up of the former is represented in Fig. 4 (b), in which it is evident that the diamond tip has penetrated well into the substrate before coating failure has occurred. Furthermore, the plastic deformation along the edges of the scratch track is evident, as is the presence of small cracks running transversely to the scratch direction.

The micrograph shown in Fig. 4 (c) shows a deeper crater over the zone of critical failure and in this case the scratch depth is easier to measure, using the same simple calculation as for the conventional film thickness. The Calotest also finds application to non-flat samples such as coated cylinders, where the coating thickness can be measured from the elliptical crater produced. A typical example is shown in Fig. 5, for a CrN coating on a machining tool. Better contrast was achieved by etching the steel substrate. The thickness of coatings deposited on spherical samples can also be measured using the Calotest method.

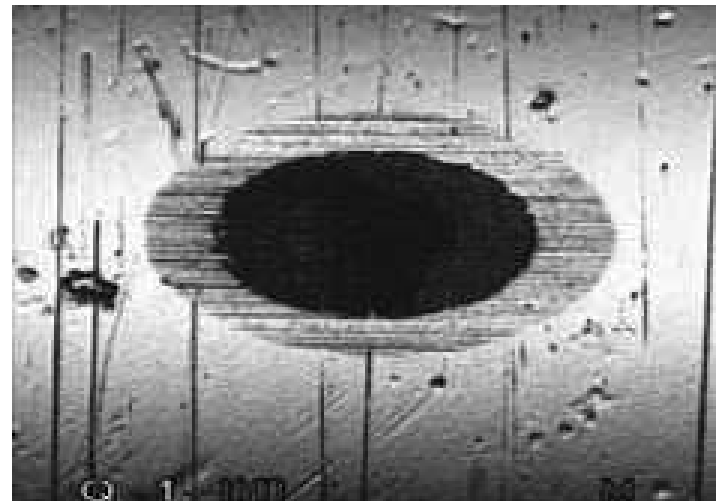


**Figure 5** : Calotest crater on a TiN coated milling bit. The cylindrical geometry of the tool means that an elliptical crater is produced, for which the longer axis has the same symmetry as a flat sample and the shorter axis the symmetry of a spherical sample.

# Combined NHT/SFM for characterisation of coated systems

## Introduction

Recent work [1] on coated systems with the NHT and integrated Scanning Force Microscope (SFM) objective has shown that the effects of pile-up have important consequences for the measurement of mechanical properties from nanoindentation load-displacement curves. This is because the calculated contact area between indenter and sample does not take into account any variation due to pile-up or sink-in of material around the indentation site.

This application note focuses on a titanium thin film of thickness 200 nm deposited onto a Si [100] substrate. Indentations have been performed using a Berkovich (three-sided) pyramidal indenter at depths from 25 nm up to 1225 nm, this being the total measurement range of the NHT instrument for this particular sample.

## Results

The plasma deposited titanium is in fact harder than the Si substrate, due to the high internal stresses produced as a result of deposition and the oxide film (usually TiO<sub>2</sub>) which forms immediately on removal of the sample from the reactor. The SFM images (Fig. 1) clearly show the surface morphology and grain structure of the deposited coating.

For the imaged indentation made with  $h_{max} = 50$  nm, the residual imprint is barely visible and is of a similar magnitude as the surface roughness ( $\sim 20$  nm). As  $h_{max}$  is increased, no apparent pile-up effects are noticeable until the substrate is reached, suggesting that plastic flow is far more restricted than that of softer coatings (such as aluminium or gold). For depths where  $h_{max} > 200$  nm (the film thickness), the amount of pile-up increases gradually but it can be observed that the surface morphology of the piled-up material remains the same as that surrounding it. This would suggest that, contrary to softer coatings where material is obviously pushed to the sides of the indenter, the material has undergone uplift due to substrate relaxation on unloading. This is further confirmed by the concave edges of the imprints.

For depths much greater than the film thickness (e.g., Fig. 1 (d)), the relative amount of pile-up is significantly smaller because a greater portion of the deformed volume is in the Si substrate. The evolution of pile-up with penetration depth is represented in Fig. 2, by plotting a selection of cross-sectional profiles through imaged imprints. At depths greater than the film thickness, the transition between the coating and substrate is clearly visible, as is the elastic relaxation of the Si substrate which gives a bulge in the profile at the interface.

The variations of hardness and modulus are plotted in Fig. 3 as a function of the maximum penetration depth,  $h_{max}$ , normalised with respect to the film thickness,  $t_f$ . For the hardness plot, a steep decrease is observed from a value approaching 16 GPa at shallow depths to approximately 11 GPa at the coating-substrate interface. For values of  $h_{max}/t_f > 1$ , the hardness decreases more gradually down to a value of 9 GPa, this being the hardness of the substrate. The greater dispersion of experimental points at shallow depths can be attributed to surface roughness effects and the varying influence of the surface oxide layer, which, for such a thin film, may well extend a significant distance into the coating. The variation in elastic modulus, shown in Fig. 3 (b), descends from 270 GPa to 140 GPa, with no apparent discontinuity as a result of the coating-substrate interface. Such results confirm the applicability of the NHT to measuring mechanical properties as a function of depth in a precise and logical manner.

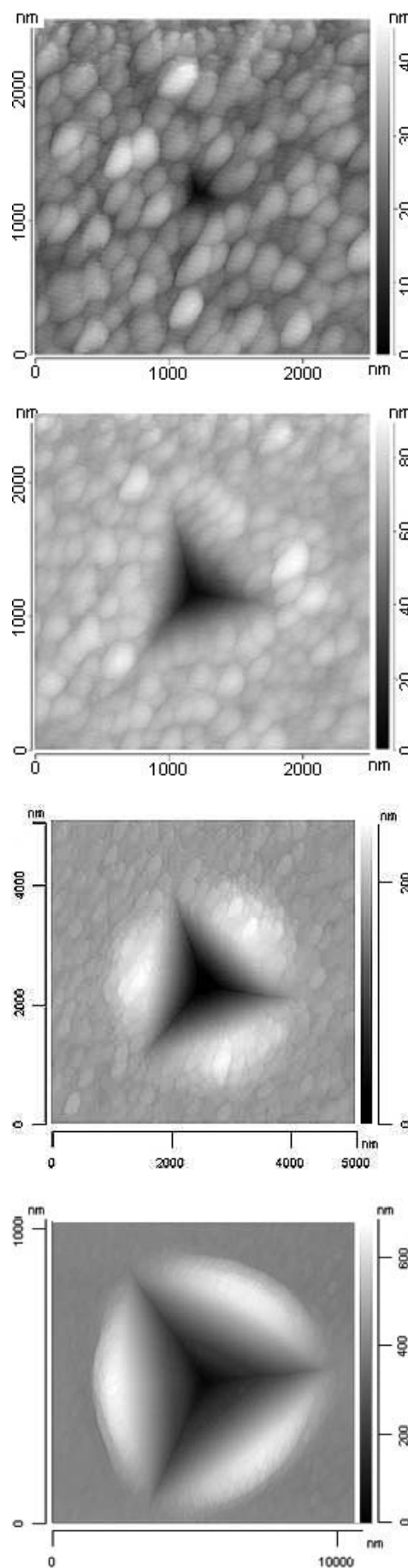


**Figure 1** : SFM images of residual imprints for maximum depths ( $h_{max}$ ) of (a) 50 nm, (b) 175 nm, (c) 400 nm, and (d) 1225 nm. The sample is a titanium film (thickness = 200 nm) sputtered onto a Si [100] substrate.

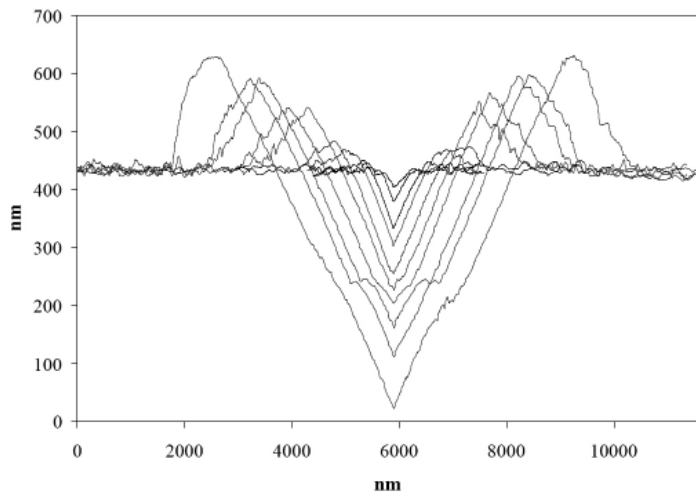


**Figure 2 :** A selection of cross-sectional profiles through imaged indentations for depths ( $h_{max}$ ) from 50 up to 1225 nm. Note the increasing influence of the Si substrate for depths exceeding the Ti film thickness (200nm).

### Conclusions

Regarding common coated systems, the NHT has proved that load-displacement information alone is not always able to determine the true deformation mechanisms occurring at the tip-sample interface, and that SFM imaging of the residual imprints at various depths is an invaluable means of characterising coating-substrate deformation behaviour.

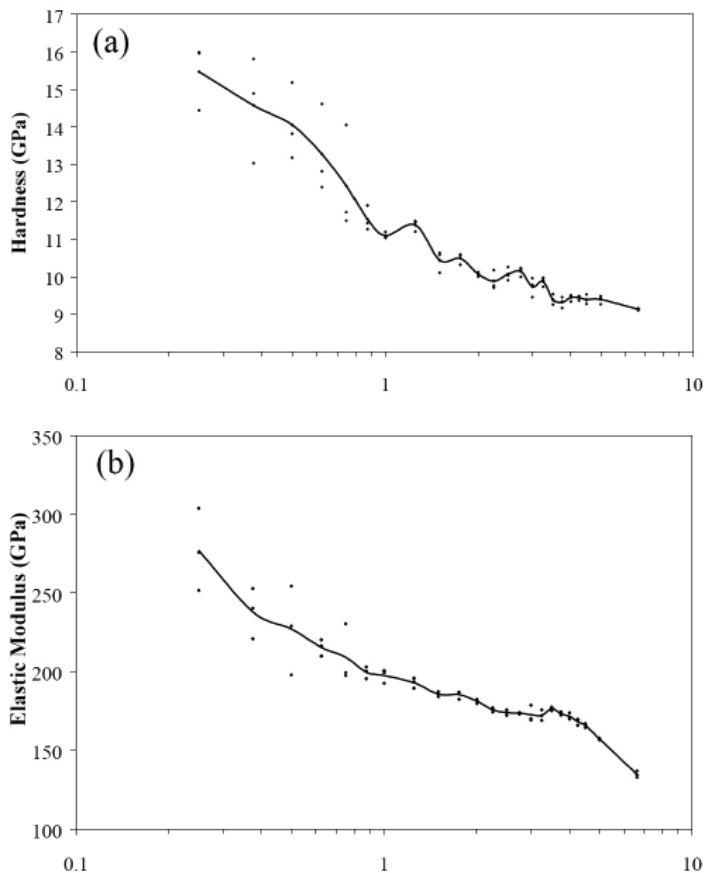


**Figure 3 :** The variation of hardness (a) and elastic modulus (b) are plotted as a function of normalised depth ( $h_{max}/t_f$ ) for a titanium film sputtered onto a Si [100] substrate

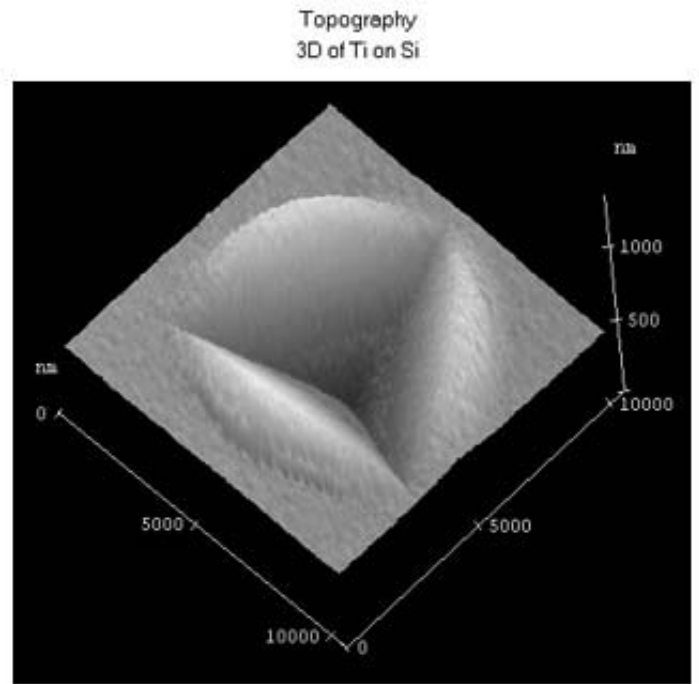


**Figure 4 :** Three-dimensional representation of the image shown in Fig. 1 (d). Note the extent of pile-up and the morphology of the Si substrate.

In addition, the NHT/SFM is capable of providing load-displacement data together with topographical information (i.e., surface roughness, extent of pile-up/sink-in effects, true area of contact, volume of material displaced, indenter tip shape, etc.) in a fast and efficient manner.

[1] N. X. Randall, Development and application of a multifunctional nanotribological tool, PhD Thesis, University of Neuchâtel, Switzerland, 1997



This Applications Bulletin is published quarterly and features interesting studies, new developments and other applications for our full range of mechanical surface testing instruments.

Editor

Dr. Nicholas Randall

Should you require further information, then please contact:

CSM Instruments  
Rue de la Gare 4  
CH-2034 Peseux  
Switzerland

Tel: + 41 32 557 5600  
Fax: +41 32 557 5610  
info@csm-instruments.com  
www.csm-instruments.com

DISTRIBUTOR: